Soft Matter

Accepted Manuscript

ROYAL SOCIETY OF CHEMISTRY

www.rsc.org/softmatter

Soft Matter

ARTICLE

Three-dimensional clustering of Janus cylinders by convex curvature and hydrophobic interactions

Jongmin Kim[a,‡], Myung Seok Oh[b,‡], Chang-Hyung Choi[a], Sung-Min Kang[a], Moo Jin Kwak[b], Jae Bem You[b], Sung Gap Im[b, *], and Chang-Soo Lee[a, *]

The three-dimensional (3D) clustering of Janus cylinders are controlled by simply tuning the cylinder geometry and hydrophobic interactions. Janus cylinders were prepared by combining two approaches: micromolding and initiated chemical vapor deposition (iCVD). Hydrophilic cylinders with a flat- or convex-top curvature were prepared by micromolding based on surface tension-induced flow. The iCVD process then provides a hydrophobic domain through the simple and precise deposition of a polymer film on the top surface, forming monodisperse Janus microcylinders. We use these Janus cylinders as building blocks to form 2D or 3D clusters via hydrophobic interactions in methanol. We investigate how cylinder geometry or degree of hydrophobic interaction affects the resulting cluster geometries. The convex-top Janus cylinders lead to 3D clustering through tip-to-tip interactions, and the flat-top Janus cylinders lead 2D clustering through face-to-face attraction. Number of Janus cylinders in 3D clusters is tuned by controlling the degree of hydrophobic (or hydrophilic) interactions.

Introduction

Self-assembly is a spontaneous process in which individual building blocks form highly ordered and complex structures driven by local interactions among the building blocks.[1-4] The formation of ordered superstructures through self-assembly of various building blocks includes molecules,[5-7] polymers[8-10] and particles.[11-17] Self-assembly using nano- and microparticles is an alternative manufacturing process that efficiently produces various materials, such as catalytic supports,[18, 19] photonic crystals for optics,[20-23] and sensors.[24] Various types of forces, such as magnetic force,[25-28] capillary force,[29-32] depletion force[33-35] and hydrophobic interaction,[36, 37] induce the self-assembly of building blocks. Among them, hydrophobic interaction is of particular interest because they control the degree of assembly relatively easily by altering the surface hydrophobicity of the particles. The local hydrophobic interaction with the environmental liquid in which the building blocks are exposed to is another important factor.[38, 39] Most studies on self-assembly driven by hydrophobic interactions have focused on submicron-scale building blocks in a bottom-up approach.[40-42] For example, spherical triblock Janus particles have been used to self-assemble in Kagome lattice structures via hydrophobic interactions between hydrophobic patches. Also, the Janus sphere has shown to produce hierarchical structures via a controlled stepwise assembly.[36, 43] These methods show great promise as submicron assembly techniques. Similarly, microparticles with patterned geometric and chemical recognition sites is also a great candidate to control self-assembly systemically with increased intricacy at the micro- or millimeter scale. A key element that remains only

vaguely understood is the control over the interaction procedures and components, such that only the desired structure is formed.[15, 38, 43, 45]

In this work, we demonstrate the 3D clustering of Janus cylinders by simply tuning the roof-top curvature and degree of hydrophobicity/hydrophilicity. Janus cylinders were prepared by micromolding integrated with initiated chemical vapor deposition (iCVD) (Scheme 1). The fabrication procedure involved two steps: 1) the synthesis of hydrophilic microcylinders by micromolding, followed by 2) the selective rendering of the hydrophobic domain on the top surface of the hydrophilic base cylinders by iCVD. We first prepared hydrophilic base cylinders with flat- or convex-top curvature through micromolding without or with addition of wetting fluids (paraffin oil), respectively. A photocurable solution composed of polyethyleneglycol diacrylate (PEG-DA) and 2-hydroxyethyl methacrylate (HEMA) was loaded into a poly(dimethylsiloxane) (PDMS) micromold. The photocurable solution was then exposed to UV light, forming cylindrical particles with flat-top curvature (Scheme 1A). Particles with convex-top curvature were fabricated upon addition of the wetting fluid and subsequent UV exposure (Scheme 1B).[46] The top surfaces of these hydrophilic microcylinders with two different shapes were readily modified by iCVD to introduce a hydrophobic domain on only the top surface of the hydrophilic cylinders, as shown in Scheme 1C.

Scheme 1. Schematic illustration of the synthesis of Janus microcylinders via micromolding combined with initiated vapor deposition (iCVD). Synthesis of the hydrophilic base cylinders using micromolds and wetting fluids: A) Flat-top cylinders and B) Convex-top cylinders. C) Selective modification of the top domains via iCVD,
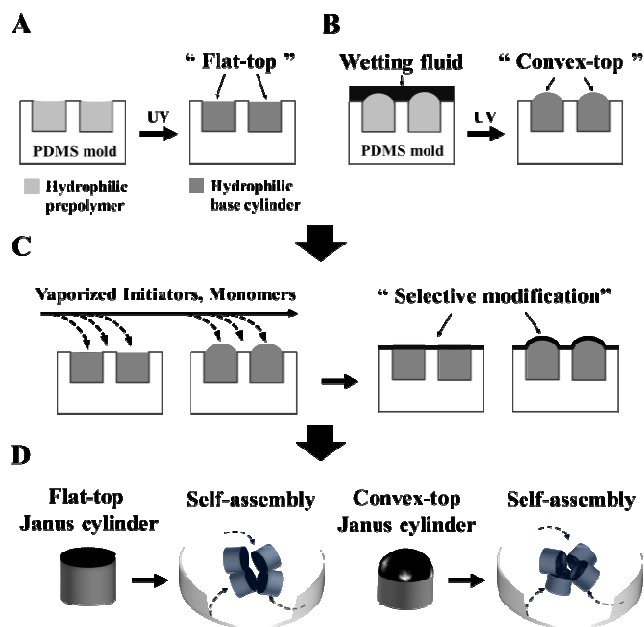
forming flat-top and convex-top Janus microcylinders. D) Self-assembly of the Janus microcylinders induced by orbital shaking.

The micromolds containing the hydrophilic cylinders were placed in an iCVD reactor, followed by exposure to various vaporized monomers (4-vinylpyridine (4VP), benzyl methacrylate (BMA), and co-flow of 4VP and BMA) and an initiator (tert-butyl peroxide). Exposure to the vapor flow selectively polymerized the top surface of the hydrophilic cylinders and formed Janus micro cylinders. After iCVD, the Janus cylinders were collected from the micromold and assembled in methanol in an orbital shaker to induce random collisions between the Janus cylinders (Scheme 1D).[39]

Experimental section

Materials

The SU-8 3025 (Photoresist) and SU-8 developers were purchased from MicroChem (Newton, MA, USA). The poly(dimethylsiloxane) (PDMS) oligomer and curing agent were purchased from Dow Corning (MI, USA). Polyethylene glycol diacrylate (PEG-DA, average Mn = 700), hydroxyethyl methacrylate (HEMA, 97%), 4-vinylpyridine (4VP, 95%), 2-hydroxy-2-methylpropiophenon (Darocur 1173, 97%), and tert-butyl peroxide (TBPO, 98%, Aldrich) were purchased from Sigma-Aldrich (MO, USA), and benzyl methacrylate (BMA, 98%) was purchased from TCI chemicals. All organic solvents such as ethylene glycol (EG), diiodomethane (DIM), paraffin oil, and methanol (MeOH) were purchased from Sigma-Aldrich (MO, USA). All chemicals were used as purchased without further purification. Deionized water (>18 Ω cm) was obtained from Milli-Q water (Milford, MA, USA).

Synthesis of microcylinders with flat and convex tops

Hydrophilic cylinders with two different shapes were synthesized from the micromolding process that was previously reported by Choi and Lee et al.[46, 47] Briefly, PDMS micromolds were prepared by conventional soft lithography.[48] The monomer solution composed of HEMA, PEG-DA and 5% darocur 1173 (v/v) was then prepared. During fabrication, the compositions of HEMA and PEG-DA were varied as 10% HEMA, 20% HEMA, 30% HEMA and 50% HEMA to control the hydrophilicity. The prepared monomer solution was gently poured onto the PDMS micromold to fill the microwells with the monomer solutions. Then, the residual solution was removed by pipette-suctioning. The loaded monomer solution was polymerized under an N_2 atmosphere by UV exposure (Inno-Cure 150, Lichtzen Co., Korea) for 5 minutes to produce hydrophilic microcylinders with flat-top surfaces. Convex-top microcylinders were synthesized by pouring paraffin oil as a wetting fluid on the surface of the monomer solution loaded in the micromolds. The interfacial tensions between the monomer solution and the wetting fluid formed the curved interface. Then, the loaded monomer solution underneath the wetting fluid was photopolymerized by UV exposure for 5 minutes to yield hydrophilic microcylinders with convex-top surfaces.

Deposition of the various iCVD polymer films

Homopolymer films (pBMA, p4VP individually) and copolymer films (pBMA-co-p4VP) were deposited on the synthesized hydrophilic microcylinders within the PDMS micromold using a custom-built iCVD reactor (Daeki Hi-Tech Co, Ltd). BMA, 4VP, and a co-monomer flow of BMA and 4VP with two different compositions were deposited on the hydrophilic cylinders. Table 1 shows the detailed deposition conditions of the individual monomer and co-monomer flows, along with the pressure, flow rate and temperature of the substrate. For the pBMA homopolymer, vaporized BMA and TBPO were introduced into the iCVD chamber at a flow rate of 0.51 and 0.60 sccm, respectively. To achieve the target flow rate, TBPO was held at room temperature, and BMA was heated to 70°C before being introduced into the iCVD reactor. The pressure of the chamber was set to 100 mTorr to maintain the fixed flow rate. The temperature of the filament was set to 200°C to activate TBPO and create radicals, and the substrate temperature was set to 40°C. The radicals then turned the monomer molecules into mPonomer radicals, inducing a chain reaction. The thickness of the polymer layer was monitored in situ by a He−Ne laser (JDS Uniphase). For the pBMA-co-p4VP copolymer, vaporized BMA, 4VP, and TBPO were introduced into the iCVD chamber.

Table 1. Deposition conditions of the iCVD polymeric layers

Controlled polymeric surfaces via iCVD	Deposition condition				
	Monomer and initiator flow rates			Pressure (mTorr)	Substrate temperature (°C)
	BMA (sccm)	4 VP (sccm)	TBPO (sccm)		
p4 VP	-	1.94	0.60	260	25
Co-1	0.51	1.94	0.60	260	32
Co-2	0.51	1.94	0.60	220	32
pBMA	0.51	0.00	0.60	100	40

The flow rates of BMA and TBPO were the same as for pBMA, and the flow rate of 4VP was 1.94 sccm. The partial pressure of 4VP was manipulated by controlling the total chamber pressure. To increase the concentration of 4VP, the total chamber pressure of Co-1 and Co-2 were set at 260 mmTorr

and 220 mmTorr, respectively. The filament temperature was set to 200°C. The substrate temperature was set to 32°C lower than that of the pBMA homopolymer to induce the adsorption of 4VP.

Self-assembly and image analysis

To induce random collisions between the Janus cylinders, an orbital shaker was used.[39] The synthesized Janus cylinders were washed with isopropyl alcohol (IPA) several times and redispersed in IPA. Then, 10 μl of Janus cylinders dispersed in IPA were loaded into the glass dish. After complete evaporation of IPA, the dishes were filled with 2 ml of methanol. The final concentration of loaded Janus cylinders was approximately 100 cylinders/ml. The dish was then sealed with Teflon tape to prevent evaporation of MeOH. Subsequently, the dish containing the Janus cylinders was stirred by an orbital shaker at 100 rpm (SHO-1D, WiseShake, Wertheim, Germany) to produce random collisions between the cylinders for 30 minutes. Finally, the assembled clusters were observed on an inverted fluorescence microscope (TE2000, Nikon, Japan) equipped with a CCD camera (Coolsnap cf, Photometrics, USA). Image Pro software (Media Cybernetics, MD, USA) and Image J software (http://rsb.info.nih.gov/ij/) were used to obtain optical fluorescent images and analyze the assembled clusters individually.

Quantitative analysis of the assembled clusters

The assembled clusters were quantitatively analyzed for the assembly yield and probability defined by the following equations below:

$$Probability\,(\%) = \frac{The\;number\;of\;all\;assembled\;\;x\text{-}mers\,(N_x)}{The\;number\;of\;all\;clusters\;(N_c)} \cdots\cdots\cdots (1)$$

where x is 2 (dimers) or 3 (trimmers), or 4 (tetramers) or 5 (pentamers) or ≥6 (more than hexamers), depending on their assembled clusters.

$$Yield\,(\%) = \frac{The\;number\;of\;assembled\;Janus\;cylinders\,(N_{JC})}{The\;total\;number\;of\;Janus\;cylinders\,(N_t)} \cdots\cdots\cdots (2)$$
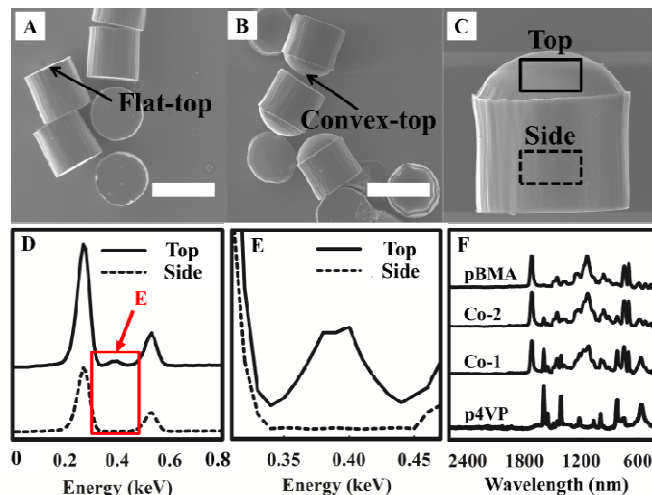
Results and discussion

Synthesized Janus microcylinders with flat and convex tops

We produced Janus cylinders with flat- or convex-top curvatures using micromolding integrated with iCVD (Scheme 1). A mixture of pHEMA and PEG-DA (3:7, v/v) was used to synthesize the hydrophilic base cylinders, and poly benzyl methacrylate (pBMA) was used to impart a hydrophobic domain on the top surface via iCVD. Scanning electron microscopy (SEM) images show highly uniform Janus cylinders with flat- and convex-top curvatures (Fig. 1A and B).

Next, energy-dispersive X-ray spectroscopy (EDX) proved that iCVD successfully imparted a hydrophobic domain on the

Fig. 1. Characterization of the synthesized Janus microcylinders. SEM images of A) flat-top and B) convex-top Janus microcylinders. C) Enlarged HR-SEM images of the convex-top Janus microcylinders. D) EDX spectrum analyzed from the top and side of the convex-top Janus microcylinders. E) The characteristic nitrogen peak on the top regions indicates that p4VP resulted from selective deposition of pBMA-co-p4VP on the Janus microcylinders. F) Fourier-transform infrared (FTIR) spectra of two different homopolymers (p4VP, pBMA) and two different copolymers composed of pBMA and p4VP (Copolymer 1, 2 (Co-1, Co-2)) deposited via iCVD; Co-1 and Co-2 were deposited using two different total pressures (Co-1: 260 mTorr and Co-2: 220 mTorr). (See experimental section)

top surface of the Janus cylinders. We individually characterized the elemental compositions of the top and side regions of the cylinders (Fig. 1C). As shown in Fig. 1D and E, the characteristic nitrogen peaks at approximately 0.4 keV (typically 0.392 keV) were only detected on the top surface of the cylinders,[49-51] clearly indicating that the iCVD pBMA-co-p4VP polymeric layer had been deposited exclusively on the desired top region of the cylinders. One of the major advantages of iCVD is the ability to control the surface chemistry using homo- and co-monomers with various chemical compositions in a single step, which was used to control the hydrophobicity of the top surface of the Janus cylinders. Here, BMA, 4VP, and a co-monomer flow of BMA and 4VP with two different compositions were deposited on the hydrophilic cylinders to demonstrate this controlled hydrophobicity (Table 1). The same polymer films were deposited on silicon substrates in the same batch as control surfaces. Presumably, the deposited polymeric layers on the silicon substrates are identical to the top surfaces of the Janus cylinders. Four different iCVD polymer films on silicon substrates were analyzed by Fourier-transform infrared (FT-IR) spectroscopy. The FT-IR spectrum of pBMA in Fig. 1F shows four characteristic peaks at 1720 cm⁻¹ and 1140 cm⁻¹ attributed to the unconjugated ester (C–CO–O–C) stretching of methacrylate.[52] Peaks at 700 cm⁻¹ and 750 cm⁻¹ were assigned to mono-substituted benzene peaks.[53] Additionally, the FT-IR spectrum of p4VP shows five characteristic peaks at 820 cm⁻¹, 1420 cm⁻¹, 1500 cm⁻¹, 1560 cm⁻¹, and 1600 cm⁻¹ corresponding to substituted pyridine.[54] All of the characteristic peaks from the pBMA and p4VP homopolymers were also observed for both copolymer 1 (Co-1) and copolymer 2 (Co-2). The chemical compositions of Co-1 and Co-2 were controlled by the flow rate of the vaporized BMA and 4VP monomers.

The characteristic peaks of Co-2 show relatively decreased pyridine absorption peaks compared to Co-1, whereas the characteristic peaks in pBMA corresponding to mono-substituted benzene increased notably. This indicates that the BMA fraction in Co-2 was higher than in Co-1 and thus more hydrophobic.

The hydrophobicity of the top surface can be systemically controlled by changing the chemical composition during iCVD.

Overall, the results shown in Fig. 1 clearly demonstrate that this simple fabrication technique produces highly uniform Janus cylinders with tunable curvatures. Compared to previous techniques for the synthesis of Janus particles, such as glancing angle deposition,[55] sinking-in,[56] and polymer entrapping methods,[57] our method offers several advantages: production of highly uniform Janus particles with tunable geometries, no need for protective layers to allow selective modification, and flexibility in the choice of chemicals for particle functionalization.

2D clustering of flat-top Janus cylinders with hydrophobicity

Clustering patterns can be tuned by controlling the degree of hydrophobic attraction, which stems from the random collisions between the Janus cylinders dispersed in methanol (Fig. 2A). To investigate the effect of the degree of attractive force for the hydrophobic domains of the resulting assembled formations, we used the Janus cylinders composed of hydrophilic base cylinders (pHEMA:PEG-DA = 30:70, v/v) and iCVD-deposited hydrophobic domains, such as the two copolymers with different ratios of BMA and 4VP (Co-1, Co-2) and pBMA. The degree of hydrophobicity characterized by the water contact angle was sequentially increased as follows: base (pHEMA:PEG (30:70, v/v) < Co-1 < Co-2 < pBMA (Fig. 2J). The flat-top Janus cylinders formed 2D clusters through face-to-face (flat-top contact area) self-assembly (Fig. 2B-E) under all conditions. Bright-field images of Fig. 2C-E show the formation of 2D clusters by self-assembly of the flat-top Janus cylinders, whereas hydrophilic base cylinders were well dispersed without any interaction between the cylinders (Fig. 2B, F). Additionally, the increase in hydrophobicity of the domains on the top surface lead to highly complex clusters consisting of tunable numbers of the particles. Specifically, the magnified bright-field images of Fig. 2G-I clearly show the formation of clusters in each cylinder's condition: dimers (N=2), trimers (N=3), and tetramers (N=4). The probability of the clusters was quantitatively analyzed from the entire population of 100 cylinders per each condition. Fig. 2K shows the distribution of clustering patterns depending on the hydrophobic domains of the Janus cylinders. The Janus cylinders with Co-1 hydrophobic domains formed dimers with 100% yield. Multiple clusters such as trimers (N=3) and tetramers (N=4) were formed from the Janus cylinders with Co-2 and pBMA hydrophobic domains. The assembly yield representing the total number of assembled clusters in methanol gradually increased because of the increased hydrophobic interaction force (Fig. 2L). Presumably, the tunable clustering resulted from the assembly configurations based on the degree of hydrophobic interactions. For example, the Janus cylinders with a pBMA domain imparted strong hydrophobic interactions. The leftover hydrophobic domains of the Janus cylinders, even after the initial assembly, enabled the sequential assembly of the cylinders onto the available hydrophobic domains to form trimers or tetramers. The Janus cylinders with less hydrophobic interactions (Co-1) required a relatively large contact area to form assembled structures, and predominantly formed dimers.

Fig. 2. 2D clusters formed from flat-top Janus microcylinders with controlled hydrophobicity. A) Schemes of self-assembly using flat-top
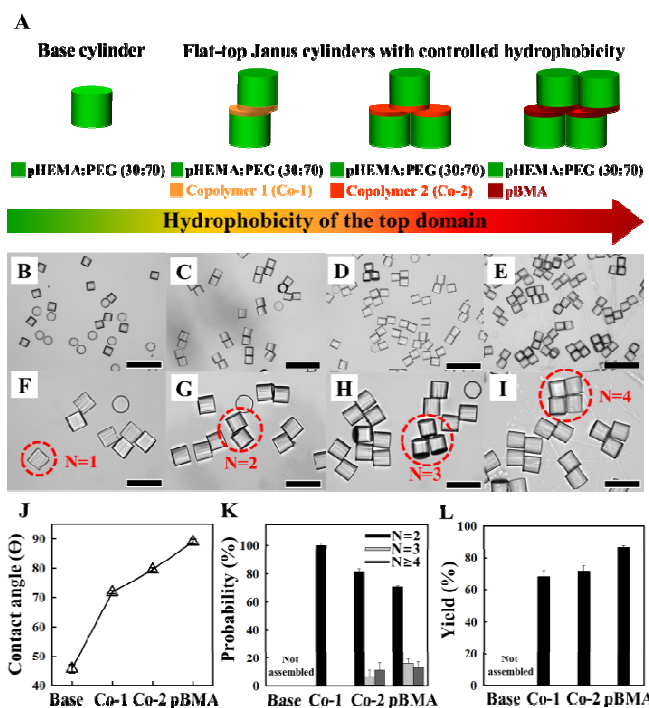
Janus microcylinders composed of three different hydrophobicities controlled via iCVD and pHEMA:PEG (30:70, v/v) for the hydrophilic base cylinders. B-I) Bright-field images of the 2D clusters; B, F) base cylinders; C, G) Co-1/pHEMA:PEG (30:70, v/v); D, H) Co-2/pHEMA:PEG (30:70, v/v); E, I) pBMA/pHEMA:PEG (30:70, v/v), respectively. Scale bars indicate 200 μm for B-E and 100 μm for F-I. J) Water contact angle of the hydrophobicity-controlled surfaces. K) Assembly probability at each number of particles and L) Assembly yield analyzed from the entire distribution of assembled clusters.

Free energy of adhesion of Janus microcylinders

The interaction force between the Janus cylinders can be evaluated in terms of the thermodynamic free energy of adhesion. We examined surface properties and free energy of adhesion between the Janus cylinders in two sequential steps: 1) determine the surface free energies of the hydrophobic domains and the hydrophilic base cylinders and 2) calculate the interfacial free energy between two different phases, and examine the adhesion free energy between each surface of Janus cylinders in methanol.

First, we examined the surface free energy of the hydrophobic domains and hydrophilic base cylinders using the van Oss-Chaudhury-Good (vOCG) equation (3) and equation (4).[58]

$$\gamma_L(1+\cos\theta)=2\sqrt{\gamma_s^{LW}\gamma_L^{LW}} + 2\sqrt{\gamma_s^+\gamma_L^-} \quad + 2\sqrt{\gamma_s^-\gamma_L^+} \cdots\cdots\cdots\cdots(3)$$

$$\gamma_s^{tot} = \gamma_s^{LW} + \gamma_s^{AB} \cdots\cdots\cdots\cdots\cdots\cdots\cdots\cdots\cdots\cdots\cdots(4)$$

$$\gamma_s^{AB} = 2\sqrt{\gamma_s^+\gamma_L^-} \cdots\cdots\cdots\cdots\cdots\cdots\cdots\cdots\cdots\cdots(5)$$

Table 2. Surface free energy and free energy of adhesion for Janus microcylinders with controlled hydrophobicity.

Polymeric surfaces		Contact angle (°)			Surface free energy components [mJ/m^2]			
		Water	DIM	EG	γ_s	γ_s^{LW}	γ_s^+	γ_s^-
Hydrophilic surface	pHEMA:PEG (30:70)[1]	45.50	23.70	20.59	49.64	46.61	0.07	32.28
Hydrophobic domains	Co-1[2]	71.78	16.21	58.30	48.80	48.80	0[3]	15.59
	Co-2[2]	79.46	8.12	59.58	50.29	50.29	0[3]	8.07
	pBMA[2]	89.00	8.00	65.00	50.31	50.31	0[3]	2.94
MeOH		-	-	-	22.5[4]	18.2[4]	0.06[4]	77[4]

Janus cylinders (Hydrophobic/Hydrophilic)[5]	Free energy of adhesion (ΔG^{ad}) [mJ/m^2]		
	Hydrophilic-Hydrophilic surfaces[6]	Hydrophilic-Hydrophobic surfaces[7]	Hydrophobic-Hydrophobic surfaces[8]
Co-1/pHEMA:PEG (30:70)	-11.13	-14.05	-19.52
Co-2/pHEMA:PEG (30:70)	-11.13	-14.29	-21.81
pBMA/pHEMA:PEG (30:70)	-11.13	-13.98	-22.90
Hydrophilic base cylinders (pHEMA:PEG (30:70))	-11.13	-	-

[1]Hydrophilic surface synthesized from photopolymerization of a mixture of HEMA and PEG-DA (30:70, v/v).
[2]Three different hydrophobic domains deposited on the hydrophilic top surface by iCVD; Two copolymers (Co-1, Co-2) and a homopolymer (pBMA) (See experimental section).
[3]Negative value was considered to be zero.[59]
[4]Values are reported in the literature.[60]
[5]Hydrophobic/Hydrophilic: Hydrophobic domains on the top surface of the hydrophilic base cylinders.
[6]ΔG^{ad} between the two identical hydrophilic surfaces (pHEMA:PEG = 30:70, v/v).
[7]ΔG^{ad} between the hydrophilic surface and the hydrophobic domains; Co-1, Co-2, and pBMA.
[8]ΔG^{ad} between the two individual hydrophobic domains.

The subscripts S and L represent solid and liquid, respectively, and the superscripts LW, AB, +, and – represent the apolar (Lifshitz-van der Waals) components, the polar components including electron-acceptors (Lewis acids), and the electron-donors (Lewis bases), respectively.

To examine the total surface free energy (γ^{tot}), each surface free energy components (γ^{LW}, γ^+, γ^-) was calculated by using equation (3), and the contact angles of three different liquids with known properties: water, diiodomethane (DIM), and ethylene glycol (EG). Then, the total surface free energy of each surface was calculated from equation (4) by using each surface free energy component (γ^{LW}, γ^+, γ^-) and equation (5).

Next, we examined the free energy of adhesion (ΔG^{ad}) between the Janus cylinders using the equation (6).[61, 62]

$$\Delta G^{ad}_{132} = \gamma_{12} - \gamma_{13} - \gamma_{23} \bullet (6)$$

where the system was composed of Janus cylinders (hydrophobic domains (phase 1)), hydrophilic base cylinders (phase 2)), and methanol as an assembly medium (phase 3). The interfacial free energies solid-liquid (γ_{13}, γ_{23}) and solid-solid (γ_{12}) interactions were determined using the surface free energy values (γ^{tot}, γ^{LW}, γ^+, γ^-) of the hydrophobic domains, hydrophilic surfaces, polar solvent (MeOH) and equation (7).[38]

$$\gamma_{ij} = \gamma_i + \gamma_j - 2\sqrt{\gamma_i^{LW}\gamma_j^{LW}} - 2\sqrt{\gamma_i^+\gamma_j^-} - 2\sqrt{\gamma_i^+\gamma_j^-} \bullet\bullet\bullet\bullet\bullet\bullet\bullet\bullet\bullet\bullet\bullet\bullet\bullet\bullet\bullet\bullet (7)$$

where γ_{ij} represents the interfacial free energy per unit area between two phases. Subsequently, the interfacial free energy was substituted in equation (6) for the evaluation of the ΔG^{ad} between the Janus cylinders.

The contact angle values on the hydrophilic surface (pHEMA:PEG (30:70, v/v)) and three different hydrophobic surfaces controlled via iCVD are summarized in Table 2. The contact angles of the hydrophilic liquids (Water, EG) on the hydrophobic pBMA domain were higher than that on the Co-1 and Co-2 surfaces. Additionally, the apolar components (γ^{LW}) of the pBMA domains were higher than that of the others, implying that hydrophobicity of the top domains was controlled by iCVD. Next, we examined the free energy of adhesion between the Janus cylinders. As the hydrophobicity of the top surfaces increased, the ΔG^{ad} between the hydrophobic surfaces decreased. The free energy between the pBMA surfaces showed the most negative value, which represents the strongest hydrophobic interaction force. The free energy of adhesion between hydrophobic domains can be controlled systemically by simply tuning the hydrophobicity of the top domains. We believe that this controlled free energy of adhesion resulted in the tunability of the assembled clusters that is discussed in Fig. 2.

2D clustering of flat-top Janus cylinders with hydrophilicity

Self-assembly of flat-top Janus cylinders was also evaluated with controlled hydrophilicity. Hydrophilicity of the building blocks can also manipulate self-assembly of amphiphilic supramolecules.[63-66] For example, formation of polymersomes is highly dependent on the length of hydrophilic block and results in fluid-like bilayer-forming vesicles or spherical micelles.[67] However, the effect of microparticle hydrophilicity on self-assembly remains unclear. We expected that the degree of hydrophilicity of Janus cylinders would play an important role in controlling microparticle self-assembly.

The hydrophilicity of Janus cylinder were modulated by changing the composition ratio of HEMA used as a hydrophilic co-monomer of the base cylinders, while the iCVD pBMA for the hydrophobic domain was fixed (Fig. 3A). As a result, the hydrophilicity of the Janus cylinders gradually increased with the increasing HEMA fraction (Fig. 3J). Typically, flat-top Janus cylinders with different hydrophilicity form 2D clusters through hydrophobic interactions (Fig. 3B-E). The 2D formation of clusters was highly dependent on hydrophilicity of the Janus cylinders. The most abundant clusters were dimers (N=2), formed by face-to-face interactions between the top surfaces of the hydrophobic pBMA domain. The other multiple clusters (N=3, 4, or higher) were formed by increasing the hydrophilicity of the Janus cylinders (Fig. 3F-I).

We statistically examined the entire formation of 2D clusters through image analysis. The probability in Fig. 3K clearly shows that the increase in the hydrophilicity of the Janus cylinders lead to an increase in numbers of the 2D clusters. The Janus cylinders composed of pHEMA and PEG (50:50, v/v) formed multiple clusters including trimers (N=3), tetramers (N=4) and greater than pentamer (N ≥ 5). Whereas, 100% dimers (N=2) were formed by the Janus cylinders composed of less hydrophilic base cylinders (pHEMA:PEG = 10:90, v/v). Also, increases in the hydrophilicity of the Janus cylinders increased the total number of assembled clusters in methanol (Fig. 3L). We believe that the hydrophilicity of the Janus cylinders likely affects the kinetics of self-assembly. Compared to the less hydrophilic Janus cylinders (pHEMA:PEG = 10:90, v/v), the most hydrophilic Janus cylinders (pHEMA:PEG = 50:50, v/v) were more readily hydrated that results in rapid exposure of hydrophilic base cylinders part to a polar solvent (methanol) for the same amount of time. This likely induces acceleration of minimizing the hydrophobic area between the Janus cylinders and results in high assembly yields, but the exact mechanism remains unclear. The increased number of cylinders in the 2D clusters is also likely induced by the hydration effect of the hydrophilic base cylinders. In molecular assembly, the increased hydrophilicity of the polar head group from increased length or size forms larger aggregates with close packing.[68-73] It is still difficult to address the direct relationship between molecules and microcylinders, but these results imply that the increased hydrophilicity of the base cylinders increased the number of particles comprising the 2D clusters.

To better understand the dependence of the Janus cylinder self-assembly on hydrophilicity, the free energy of adhesion between the Janus cylinders was examined. First, we measured the contact angles of the different liquids on four different hydrophilic surfaces and the pBMA surface. Subsequently, the interfacial free energy and the adhesion free energy were examined using equation (3-6). The contact angles and the surface free energies of the four different hydrophilic surfaces
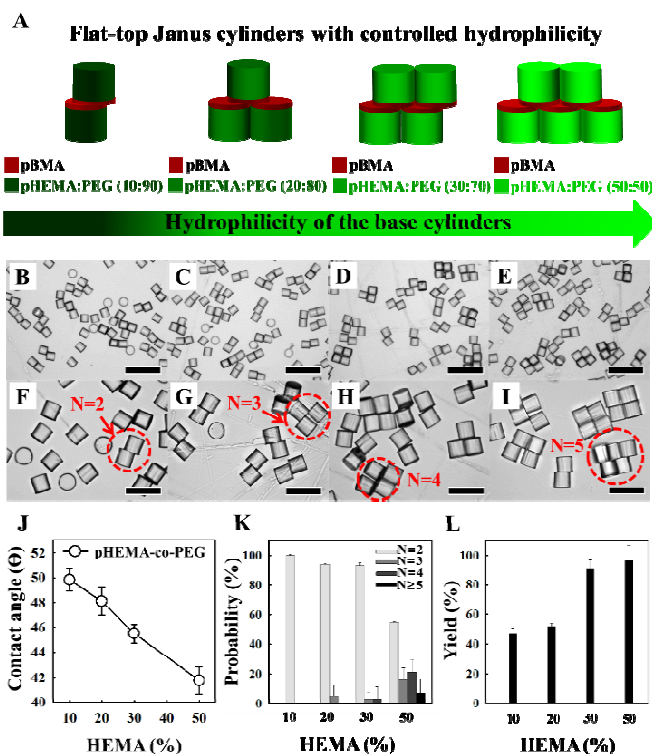

Fig 3. 2D clusters formed by flat-top Janus microcylinders with controlled hydrophilicity. A) Evolution of self-assembly using flat-top Janus microcylinders composed of pBMA for the hydrophobic domains and four different hydrophilic base cylinders controlled by the ratio of HEMA to PEG-DA. B-I) Bright-field images of the 2D clusters formed by flat-top Janus microcylinders: B, F) pBMA/pHEMA:PEG (10:90, v/v); C, G) pBMA/pHEMA:PEG (20:80, v/v); D, H) pBMA/pHEMA:PEG (30:70, v/v); E, I) pBMA/pHEMA:PEG (50:50, v/v). Scale bars indicate 200 μm for B-E and 100 μm for F-I. J) Water contact angles on the hydrophilicity-controlled surfaces. K) Assembly probability for each number of particles. L) Assembly yield analyzed from the entire distribution of assembled clusters.

and the pBMA hydrophobic surface are summarized in Table 3.The contact angles of the polar liquids (Water, EG) on the hydrophilic surfaces decreased as the ratio of HEMA increased, while the contact angles of the apolar liquid (DIM) increased. The surface free energy of the base component on the hydrophilic surfaces increased slightly because of the increase in the ratio of HEMA, indicating that the hydrophilicity of the Janus cylinders was precisely controlled.

In terms of the adhesion free energy between the Janus cylinders, the ΔG^{ad} between the hydrophilic surfaces increased as the ratio of HEMA increased. The ΔG^{ad} between pHEMA:PEG (50:50, v/v) surfaces was higher than that of pHEMA:PEG (10:90, v/v) surfaces, which indicates that pHEMA:PEG (50:50, v/v) was more readily hydrated by the polar solvent.

As discussed in Figure 3, the polar head groups or hydrophilic blocks of the molecular assembly played a significant role in determining the final assembled structures because of the hydration effect.[69-74] Similarly, the different degrees of hydration on the hydrophilic surface of the Janus cylinders likely enabled the tunability in the final assembled clusters. Designing controlled 2D clusters with flat-top Janus cylinders with tunable hydrophobicity and hydrophilicity are a novel addition to the previous reports on self-assembled clusters from Janus particles with controlled sizes of

Table 3. The surface free energy and free energy of adhesion for Janus microcylinders with controlled hydrophilicity.

Polymeric surfaces		Contact angle (°)			Surface free energy components [mJ/m^2]			
		Water	DIM	EG	γ_s	γ_s^{LW}	γ_s^+	γ_s^-
Hydrophilic surfaces	pHEMA:PEG (10:90)[1]	49.82	17.60	31.76	48.45	48.45	0[2]	30.60
	pHEMA:PEG (20:80)[1]	48.11	22.50	26.02	48.50	47.01	0.02	30.77
	pHEMA:PEG (30:70)[1]	45.50	23.70	20.59	49.64	46.61	0.07	32.28
	pHEMA:PEG (50:50)[1]	41.75	24.50	16.64	49.88	46.33	0.09	35.96
Hydrophobic domains	pBMA	89.00	8.00	65.00	50.31	50.31	0[2]	2.94
MeOH		-	-	-	22.5	18.2	0.06	77

Janus cylinders (Hydrophobic/Hydrophilic)	Free energy of adhesion (ΔG^{ad}) [mJ/m^2]		
	Hydrophilic-Hydrophilic surfaces[3]	Hydrophilic-Hydrophobic Surfaces[4]	Hydrophobic-Hydrophobic Surfaces[5]
pBMA/pHEMA:PEG (10:90)	-17.70	-20.28	-22.90
pBMA/pHEMA:PEG (20:80)	-14.84	-17.78	-22.90
pBMA/pHEMA:PEG (30:70)	-12.84	-15.68	-22.90
pBMA/pHEMA:PEG (50:50)	-12.33	-15.00	-22.90

[1]Increase in hydrophilicity by varying the mixing ratio of HEMA and PEG-DA (v/v) (See experimental section).
[2]Negative value was considered to be zero.[59]
[3]ΔG^{ad} between the individual hydrophilic surfaces.
[4]ΔG^{ad} between the four individual hydrophilic surfaces and the hydrophobic pBMA domains.
[5]ΔG^{ad} between the identical hydrophobic pBMA domains.

hydrophobic patches or ratios of hydrophobic blocks[36, 75].

The hydrophobic interactions between the flat-top surfaces guides the directional assembly of the Janus cylinders. This geometry-driven directional assembly forms the 2D clusters, whose complexity can be changed simply by tuning either the hydrophobicity of the top surface and/or the hydrophilicity of the base cylinders.

In short summary, the flat-top Janus cylinders can be assembled into 2D clusters using face-to-face hydrophobic interactions (Figure 2 and 3). The number of cylinders comprising the 2D clusters and its assembly yield can also be easily tuned by controlling the hydrophobicity of the top surface and the hydrophilicity of the base cylinders.

3D clustering of convex-top Janus cylinders with hydrophobicity

Self-assembly of convex-top Janus cylinders was also controlled by hydrophobicity. A major issue in designing building blocks for self-assembly is controlling surface chemistry and geometry. For example, optically active materials are fabricated via surface tension and complementary shape-induced self-assembly.[76, 77] Therefore, fabrication of microparticles with controlled geometries and chemical properties could potentially expand the design varieties of self-assembly.

Convex-top Janus cylinders composed of 50% pHEMA and 50% PEG as hydrophilic base cylinders and three different hydrophobic domains were used for self-assembly. The three different hydrophobic domains were the same as in the assembly of the flat-top Janus cylinders: Co-1, Co-2, and pBMA (Figure 2J). The bright-field images show that the overall distribution of the 3D clusters of the convex-top Janus cylinders formed through hydrophobic interactions (Figure 4C-E). No interactions were observed during the self-assembly experiment with the base cylinders as a control (Figure 4B, F). The assembled 3D clusters were formed through tip-to-tip interactions (localized contact areas) between the hydrophobic domains of the convex-top geometry. The number of particles in these 3D clusters was tuned depending on the hydrophobicity of the top domains (Figure 4G-I). Small clusters were formed by convex-top Janus cylinders with relatively less hydrophobicity (Co-1, and Co-2), and large clusters with dense packing were formed by convex-top Janus cylinders with the strongest hydrophobicity (pBMA). The entire distribution of these 3D clusters was quantitatively analyzed (Figure 4J). The probability clearly showed that the number of particles in the 3D clusters was highly tunable by controlling the hydrophobicity. For the Janus cylinders (Co-1) with relatively weak hydrophobicity, dimers (N=2) and trimers (N=3) were formed as the major clusters, whereas the majority of the clusters formed by Janus cylinders (pBMA) with the strongest hydrophobicity were pentamers (N=5) and highly complex clusters (N ≥ 6). The total number of assembled clusters in methanol representing assembly yield gradually increased with the hydrophobicity of the domains because of the increase in free energy of adhesion, as discussed in Table 2.
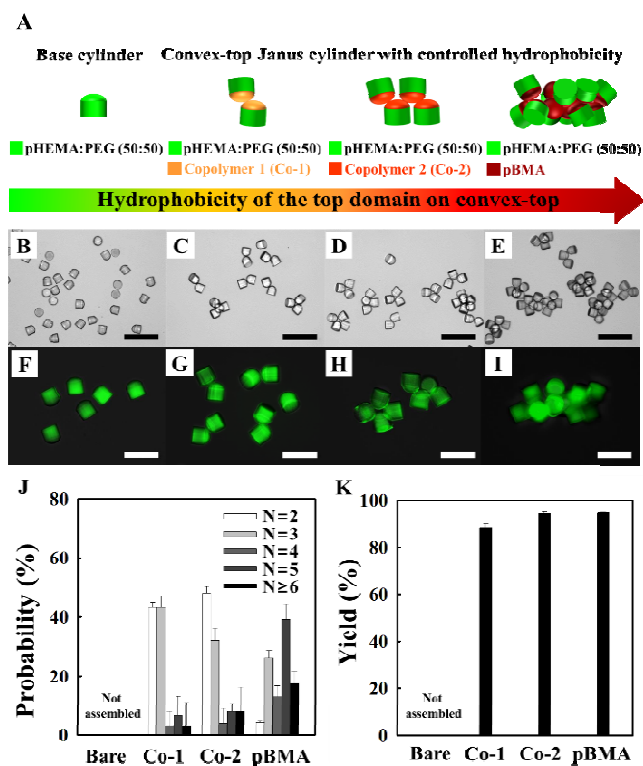
Fig 4. 3D clusters formed by the convex-top Janus microcylinders with controlled hydrophobicities. A) Schemes of self-assembly using convex-top Janus microcylinders composed of three different hydrophobic domains and a hydrophilic base cylinder (pHEMA:PEG = 50:50, v/v). B-E) Bright-field and F-I) fluorescence images of 3D-cluster formation depending on the hydrophobicity of the convex-top Janus microcylinders; B, F) Hydrophilic base cylinders as a control; C, G) Co-1/pHEMA:PEG (50:50, v/v); D, H) Co-2/pHEMA:PEG (50:50, v/v), and E, I) pBMA/pHEMA:PEG (50:50, v/v). Scale bars indicate 200 µm for bright-field images and 100 µm for fluorescence images. J) Assembly probability for each number of particles and K) Assembly yield analyzed from the entire distribution of assembled clusters.

Compared to the flat-top Janus cylinders forming 2D clusters, the convex-top Janus cylinders formed 3D with high packing densities. This can likely be attributed to the combined effects of geometry and chemical properties. The tip-to-tip interactions provided a localized contact area that was much smaller than that of the face-to-face interactions. Through this localized contact, small clusters were initially formed. In this state, there are still many remaining hydrophobic areas in the pre-formed small clusters that can potentially interact with other individual Janus cylinders. This environment favors continuous cluster growth. The equilibrium states exhibited by the final assembled clusters were determined by the hydrophobicity. For example, pBMA was the most hydrophobic surface permitted the lowest free energy of adhesion between the Janus cylinders, leading to formation of 3D clusters with high packing density. For Co-1 and Co-2 (relatively weak hydrophobic interactions), formation of small clusters, such as dimers or trimers, is thermodynamically favorable and considered an equilibrium state, even though hydrophobic areas remain.

Overall, the results described in Figure 4 indicate that the final structure of the assembled clusters can be designed by altering the geometry (convex) and chemistry (hydrophobicity) of the Janus cylinders.

Conclusions

2D and 3D clusters of Janus microcylinders were tunable by altering particle geometries and the degree of hydrophobicity/hydrophilicity. Micromolding combined with iCVD formed uniform Janus cylinders with tunable geometric and chemical properties. Flat-top Janus cylinders formed 2D clusters, whose self-assembly strongly depended on the hydrophobicity of the top domains (interaction recognition site) and the hydrophilicity of the base cylinders (interaction modulation site). Convex-top Janus cylinders assembled into complex 3D clusters with tunable numbers of particles, depending on the hydrophobicity of the top domain. The geometry and chemical properties of the Janus cylinders are important design factors for directional assembly. The effects of geometry and surface chemistry on the self-assembly of cylinders investigated in this work will further the development of new microparticle assembly designs.

Acknowledgements

Notes and references

a Department of Chemical Engineering, Chungnam National University, Yuseong-gu, Daejeon 305-764, Republic of Korea, E-mail: rhadum@cnu.ac.kr; Tel: +82-42-821-5896.
b Department of Chemical and Biomolecular Engineering and KI for NanoCentury, Korea Advanced Institute of Science and Technology, Yuseong-gu, Daejeon 305-701, Republic of Korea, E-mail: sgim@kaist.ac.kr; Tel: +82-42-350-3936.

‡ J. Kim. and M. -S. Oh contributed equally to this work.

1. R. J. Hickey, A. S. Haynes, J. M. Kikkawa and S.-J. Park, *JACS*, 2011, **133**, 1517-1525.
2. Y. Min, M. Akbulut, K. Kristiansen, Y. Golan and J. Israelachvili, *Nat. Mater.*, 2008, **7**, 527-538.
3. G. M. Whitesides and B. Grzybowski, *Science*, 2002, **295**, 2418-2421.
4. P. Yin, H. M. Choi, C. R. Calvert and N. A. Pierce, *Nature*, 2008, **451**, 318-322.
5. T. Kunitake and Y. Okahata, *JACS*, 1977, **99**, 3860-3861.
6. H. Ringsdorf, B. Schlarb and J. Venzmer, *Angew. Chem. Int. Ed.*, 1988, **27**, 113-158.
7. L.-J. Wan, *Acc. Chem. Res.*, 2006, **39**, 334-342.
8. P. Alexandridis, *Curr. Opin. Colloid Interface Sci.*, 1996, **1**, 490-501.
9. D. Chen and M. Jiang, *Acc. Chem. Res.*, 2005, **38**, 494-502.
10. G. Riess, *Prog. Polym. Sci.*, 2003, **28**, 1107-1170.
11. T. Blättler, A. Binkert, M. Zimmermann, M. Textor, J. Vörös and E. Reimhult, *Nanotechnology*, 2008, **19**, 075301-075311.
12. A. K. Boal, F. Ilhan, J. E. DeRouchey, T. Thurn-Albrecht, T. P. Russell and V. M. Rotello, *Nature*, 2000, **404**, 746-748.

13. W. Lee, H. Amini, H. A. Stone and D. Di Carlo, *PNAS*, 2010, **107**, 22413-22418.

14. M. Li, H. Schnablegger and S. Mann, *Nature*, 1999, **402**, 393-395.

15. Z. Zhang and S. C. Glotzer, *Nano Lett.*, 2004, **4**, 1407-1413.

16. Y.-S. Cho, J. W. Moon, D. C. Lim and Y. D. Kim, *Korean J. Chem. Eng.*, 2013, **30**, 1142-1152.

17. D. Dendukuri, T. A. Hatton and P. S. Doyle, *Langmuir*, 2007, **23**, 4669-4674.

18. J. Park, E. Kang, S. U. Son, H. M. Park, M. K. Lee, J. Kim, K. W. Kim, H. J. Noh, J. H. Park and C. J. Bae, *Adv. Mater.*, 2005, **17**, 429-434.

19. S. Zhang, L. Chen, S. Zhou, D. Zhao and L. Wu, *Chem. Mater.*, 2010, **22**, 3433-3440.

20. A.-P. Hynninen, J. H. Thijssen, E. C. Vermolen, M. Dijkstra and A. Van Blaaderen, *Nat. Mater.*, 2007, **6**, 202-205.

21. Y. Xia, B. Gates and Z. Y. Li, *Adv. Mater.*, 2001, **13**, 409-413.

22. S. H. Kim, W. C. Jeong, H. Hwang and S. M. Yang, *Angew. Chem. Int. Ed.*, 2011, **50**, 11649-11653.

23. S. H. Kim, H. S. Park, J. H. Choi, J. W. Shim and S. M. Yang, *Adv. Mater.*, 2010, **22**, 946-950.

24. A. S. Rad, M. Jahanshahi, M. Ardjmand and A.-A. Safekordi, *Korean J. Chem. Eng.*, 2012, **29**, 1766-1770.

25. S. Y. Lee and S. Yang, *Angew. Chem. Int. Ed.*, 2013, **52**, 8160-8164.

26. J. Yan, M. Bloom, S. C. Bae, E. Luijten and S. Granick, *Nature*, 2012, **491**, 578-581.

27. J. P. Rich, G. H. McKinley and P. S. Doyle, *Langmuir*, 2012, **28**, 3683-3689.

28. P. Panda, K. W. Bong, T. A. Hatton and P. S. Doyle, *Langmuir*, 2011, **27**, 13428-13435.

29. N. Bowden, I. S. Choi, B. A. Grzybowski and G. M. Whitesides, *JACS*, 1999, **121**, 5373-5391.

30. U. Srinivasan, D. Liepmann and R. T. Howe, *J. Microelectromech. S.*, 2001, **10**, 17-24.

31. B. J. Park, C.-H. Choi, S.-M. Kang, K. E. Tettey, C.-S. Lee and D. Lee, *Langmuir*, 2013, **29**, 1841-1849.

32. B. J. Park, C.-H. Choi, S.-M. Kang, K. E. Tettey, C.-S. Lee and D. Lee, *Soft Matter*, 2013, **9**, 3383-3388.

33. K. Zhao and T. G. Mason, *Phys. Rev. Lett.*, 2007, **99**, 268301.

34. C. J. Hernandez and T. G. Mason, *J. Phys. Chem. C*, 2007, **111**, 4477-4480.

35. D. J. Kraft, R. Ni, F. Smallenburg, M. Hermes, K. Yoon, D. A. Weitz, A. van Blaaderen, J. Groenewold, M. Dijkstra and W. K. Kegel, *PNAS*, 2012, **109**, 10787-10792.

36. Q. Chen, S. C. Bae and S. Granick, *JACS*, 2012, **134**, 11080-11083.

37. L. Hong, A. Cacciuto, E. Luijten and S. Granick, *Langmuir*, 2008, **24**, 621-625.

38. H. Onoe, K. Matsumoto and I. Shimoyama, *J. Microelectromech. S.*, 2004, **13**, 603-611.

39. H. Onoe, K. Matsumoto and I. Shimoyama, *Small*, 2007, **3**, 1383-1389.

40. G. Subramanian, V. N. Manoharan, J. D. Thorne and D. J. Pine, *Adv. Mater.*, 1999, **11**, 1261-1265.

41. Y. Xia, Y. Yin, Y. Lu and J. McLellan, *Adv. Funct. Mater.*, 2003, **13**, 907-918.

42. J. Zhang, Y. Li, X. Zhang and B. Yang, *Adv. Mater.*, 2010, **22**, 4249-4269.

43. Q. Chen, S. C. Bae and S. Granick, *Nature*, 2011, **469**, 381-384.

44. T. G. Leong, A. M. Zarafshar and D. H. Gracias, *Small*, 2010, **6**, 792-806.

45. A. Taleb, C. Petit and M. Pileni, *J. Phys. Chem. B*, 1998, **102**, 2214-2220.

46. C. H. Choi, J. Lee, K. Yoon, A. Tripathi, H. A. Stone, D. A. Weitz and C. S. Lee, *Angew. Chem.*, 2010, **122**, 7914-7918.

47. J. Jae-Min, S. Jung-Woo, C. Chang-Hyung and L. Chang-Soo, *Clean Technology*, 2012, **18**, 295-300.

48. D. C. Duffy, J. C. McDonald, O. J. Schueller and G. M. Whitesides, *Anal. Chem.*, 1998, **70**, 4974-4984.

49. N. Giambro, K. Prostak and P. Denbesten, *Caries. Res.*, 1995, **29**, 251-257.

50. L. Xue, M. Islam, A. K. Koul, M. Bibby and W. Wallace, *Adv. Perform. Matter.*, 1997, **4**, 389-408.

51. J. Wang, X. Zhang, C. Parrado and G. Rivas, *Electrochem. Commun.*, 1999, **1**, 197-202.

52. K. K. Lau and K. K. Gleason, *Macromolecules*, 2006, **39**, 3688-3694.

53. T. K. Mandal, M. S. Fleming and D. R. Walt, *Chem. Mater.*, 2000, **12**, 3481-3487.

54. J. B. You, S. Y. Kim, Y. J. Park, Y. G. Ko and S. G. Im, *Langmuir*, 2014, **30**, 916-921.

55. A. B. Pawar and I. Kretzschmar, *Langmuir*, 2008, **24**, 355-358.

56. C.-C. Lin, C.-W. Liao, Y.-C. Chao and C. Kuo, *ACS Appl. Mater. Interfaces.*, 2010, **2**, 3185-3191.

57. X. Y. Ling, I. Y. Phang, C. Acikgoz, M. D. Yilmaz, M. A. Hempenius, G. J. Vancso and J. Huskens, *Angew. Chem.*, 2009, **121**, 7813-7818.

58. C. J. Van Oss, M. K. Chaudhury and R. J. Good, *Chem. Rev.*, 1988, **88**, 927-941.

59. R. J. Good, *"Contact angle, wetting, and adhesion: A critical review,"* in Contact Angle, Wettability and Adhesion, K. L. Mittal, Ed.*, 1993.

60. C. Van Oss, *Interfacial Forces in Aqueous Media*, Marcel Decker Inc., New York, 1994.

61. C. Van Oss, R. Good and M. Chaudhury, *J. Colloid Interface Sci.*, 1986, **111**, 378-390.

62. C. Van Oss, R. Good and M. Chaudhury, *Langmuir*, 1988, **4**, 884-891.

63. M. Lee, B. K. Cho and W. C. Zin, *Chem. Rev.*, 2001, **101**, 3869-3892.

64. V. Percec, A. E. Dulcey, V. S. K. Balagurusamy, Y. Miura, J. Smidrkal, M. Peterca, S. Nummelin, U. Edlund, S. D. Hudson, P. A. Heiney, D. A. Hu, S. N. Magonov and S. A. Vinogradov, *Nature*, 2004, **430**, 764-768.

65. M. A. Alam, Y. S. Kim, S. Ogawa, A. Tsuda, N. Ishii and T. Aida, *Angew. Chem. Int. Edit.*, 2008, **47**, 2070-2073.

66. J. A. A. W. Elemans, A. E. Rowan and R. J. M. Nolte, *J Mater Chem*, 2003, **13**, 2661-2670.

67. D. E. Discher and A. Eisenberg, *Science*, 2002, **297**, 967-973.

68. A. Choucair, C. Lavigueur and A. Eisenberg, *Langmuir*, 2004, **20**, 3894-3900.

69. S. Svenson, *Curr. Opin. Colloid Interface Sci.*, 2004, **9**, 201-212.

70. A. Carlsen and S. Lecommandoux, *Curr. Opin. Colloid Interface Sci.*, 2009, **14**, 329-339.

71. K. Letchford and H. Burt, *Eur. J. Pharm. Biopharm.*, 2007, **65**, 259-269.
72. T. Gore, Y. Dori, Y. Talmon, M. Tirrell and H. Bianco-Peled, *Langmuir*, 2001, **17**, 5352-5360.
73. R. Nagarajan and E. Ruckenstein, *Langmuir*, 1991, **7**, 2934-2969.
74. A. Choucair, C. Lavigueur and A. Eisenberg, *Langmuir*, 2004, **20**, 3894-3900.
75. S. Park, J.-H. Lim, S.-W. Chung and C. A. Mirkin, *Science*, 2004, **303**, 348-351.
76. A. Terfort and G. M. Whitesides, *Adv. Mater.*, 1998, **10**, 470-473.
77. M. Boncheva and G. M. Whitesides, *Mrs. Bull.*, 2005, **30**, 736-742.

"For table of contents use only"

Jongmin Kim[a,‡], Myung Seok Oh[b,‡], Chang-Hyung Choi[a], Sung-Min Kang[a], Moo Jin Kwak[b], Jae Bem You[b], Sung Gap Im[b, *], and Chang-Soo Lee[a, *]
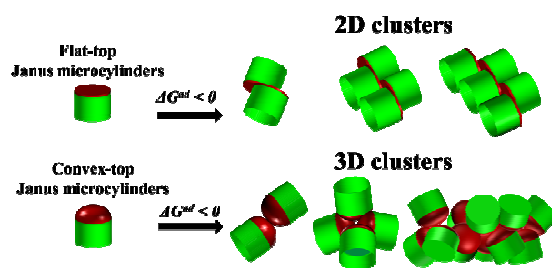
The geometry or degree of hydrophobic interaction in Janus microcylinders affects the formation of assembled structure.